JOURNAL OF APPLIED ELECTROCHEMISTRY **28** (1998) 283–288

Use of effective conductivities and unit cell-based supraelements in the numerical simulation of solid oxide fuel cell stacks*

H. KAROLIUSSEN, K. NISANCIOGLU

Department of Electrochemistry, Norwegian University of Science and Technology, N-7034 Trondheim, Norway

A. SOLHEIM

SINTEF Materials Technology, N-7034 Trondheim, Norway

Received 25 January 1997; revised 24 February 1997

The numerical simulation of current and temperature distribution in monolithic solid oxide fuel cell (SOFC) stacks requires fast computers because of the large number of mesh points required in casting a complex solid geometry into a finite difference form and the necessity to solve coupled, nonlinear differential equations. By analogy with the modelling of radiative heat transfer in packed bed reactors, a significant degree of simplification is achieved by defining effective electric and thermal conductivities for the repeating unit cell elements, identified as the basic building blocks of the SOFC stack. The effective conductivities are approximated by closed form formulae derived from the principles of electrostatics and heat conduction. The effect of radiation across the gas channels is incorporated into the expressions for the effective thermal conductivity. Using this approach, the unit cell geometry, local mass transfer processes and reaction kinetics are expressed in terms of a supraelement model in a finite difference grid for the numerical calculation of temperature and potential distributions in a stack by an iterative process. The simplifications thus provided render simulations of three-dimensional SOFC stacks tractable for desktop processors. By using the foregoing approach to numerical simulation, a parametric study of a cross-flow type SOFC is presented, and some of the results are compared with the available experimental data

Keywords: *current distribution*, *heat and mass transfer*, *radiation*, *modelling*, *experimental validation*

List of symbols

A_c unit half-cell cross-sectional area perpendicular to the direction of heat flow (m^2)
A_j cross-sectional area of element perpendicular to the direction of heat conduction (m^2)
A_w channel wall area of unit cell perpendicular to heat flow (m^2)
F geometric view factor
j element index
l_j dimension of element in the direction of heat conduction (m)
k thermal conductivity ($W\,m^{-1}\,K^{-1}$)
k^o thermal conductivity of solid at the element temperature T_j ($W\,m^{-1}\,K^{-1}$)
R_j thermal resistance of element defined by Equations 2 and 3 ($K\,W^{-1}$)
T_j element temperature (K)
V^o volume fraction of a half cell with respect to total unit cell volume
V^s volume fraction of the solid in the half cell

Greek symbols
ε emissivity
σ Stefan–Boltzmann constant ($5.670\,32 \times 10^{-8}$ $W\,m^{-2}\,K^{-4}$)

1. Introduction

Most of the current R&D work on SOFCs is centred around the monolithic or planar stack concepts because such designs are expected to yield high outputs and efficiencies, as well as low fabrication costs, relative to the earlier tubular or in-series connected plate designs. However, these improvements are achieved at the expense of an increased geometric and operational complexity. One of the most significant improvements is the design of the interconnector or bipolar plates which, while providing the channels for the gas streams, allow the passage of high current densities in short parallel paths along the stack and across thin cell plates. Moreover, shorter heat and charge conduction paths cause a more intimate cou-

*This paper was presented at the Fourth European Symposium on Electrochemical Engineering, Prague, 28–30 August 1996.

0021-891X

pling of the heat, mass and charge transport processes. The interest in using natural gas as the fuel with *in situ* reforming in the stack has further increased the design variables.

As a result of these complications, an intuitive approach to the design of such cells has become impossible. Therefore, three-dimensional numerical simulation of planar cell stacks has increasingly been used in recent design work. Modelling for design is useful for cell optimization, as well as an advanced tool for book keeping purposes in view of the large number of parameters involved, of which only a small fraction can be controlled externally. Thus, since monitoring of stack temperature, plate voltages and current distributions, internal flow rates and gas compositions is difficult, numerical models are becoming in demand for predicting these parameters under operating conditions, for trouble-shooting and maintenance purposes.

Furthermore, the complexity of the problem requires the use of large and fast computers for the finite difference representation of the geometry by a large number of mesh points and for solving the coupled partial differential equations describing various transport phenomena. This paper reviews briefly the theoretical framework of stack modelling and the numerical method, along with simplifications which can be introduced such that the numerical simulation becomes tractable for desktop processors. In particular, the development and use of supraelements based on the unit cell geometry and the definition of effective electric and thermal conductivities are discussed. A benchmark simulation case study is presented, and the simulated results are compared with data available from a simultaneous experimental program.

2. General approach to SOFC stack modelling

A mathematical model must include a set of equations which describe the following processes:

(i) Gas phase hydrodynamics.
(ii) Material balances for the components in the fuel and air phases.
(iii) As an integral part of these material balances, rate expressions for the chemical and electrochemical reactions occurring at the electrodes and electrode–electrolyte interfaces, such as methane reforming, oxidation of hydrogen and carbon monoxide at the anode– electrolyte interface, and reduction of oxygen at the cathode–electrolyte interface.
(iv) Energy balances for the gas and solid phases including heat production by reaction, convection, conduction, radiation and interfacial heat transfer.
(v) Charge balance for the solid including potential and current distributions.
(vi) Boundary conditions including compositions, mass fluxes and temperatures at inlets to stack and heat losses to an external manifold or casing by radiation.
(vii) Data base for reaction kinetics and physical and thermodynamic properties of the solid cell components as well as the components of the reactant and exhaust gas streams as a function of temperature.

Mathematical formulations of the above physicochemical phenomena have been widely discussed (e.g., [1, 2]) and therefore will not be further elaborated here.

3. Simplifications for numerical computation

A rigorous approach to numerical computation would require at least four cascaded iteration loops, taking care of gas phase hydrodynamics, material balances, the energy balance and the potential/current distribution. In addition, the complexity of the solid geometry would require a fine finite difference grid consisting of at least 45 mesh points for a typical unit cell geometry as shown in Fig. 1 for executing the temperature and current distribution calculations. For stacks consisting of thousands of such unit cells, a rigorous numerical simulation becomes a formidable task even with the use of large main frame computers, and simplification of the routines becomes necessary.

As a first simplification, the fully-developed solutions to the Navier–Stokes equations are adequate for gas flow hydrodynamics at the temperatures of interest. As a result, interfacial heat transfer at the gas–solid interfaces can be estimated by use of universal Nusselt number correlations.

In writing the equation of energy for the solid, the bipolar plate and the cell components can be considered as a nonisotropic continuum exhibiting a different effective thermal conductivity for each component of conductive heat flux. These conductivities incorporate the different solid cross section and solid-gas interfacial area experienced by each component of conductive flux. Furthermore, cross-channel radiation is an important contribution to heat transfer in the stack because the emissivities of the ceramic components are expected to be appreciable. Rather than including the radiative flux as a separate term in the usual manner, this contribution can be incorporated into the conductive terms of the equation of energy for the solid by modifying the effective conductivities.

The symmetry of the solid and linearity of the equation of energy for the solid suggest certain simplifications in expressing the effective conductivities by a semianalytic approach, involving the use of equivalent resistive networks for flow of heat. To derive an expression for the equivalent conductivity along a horizontal cell plate, for example, the unit cell in Fig. 1 can be cast into a small network of thermally resistive elements as indicated in Fig. 2(a), where the anodic and cathodic compartments of the cell are

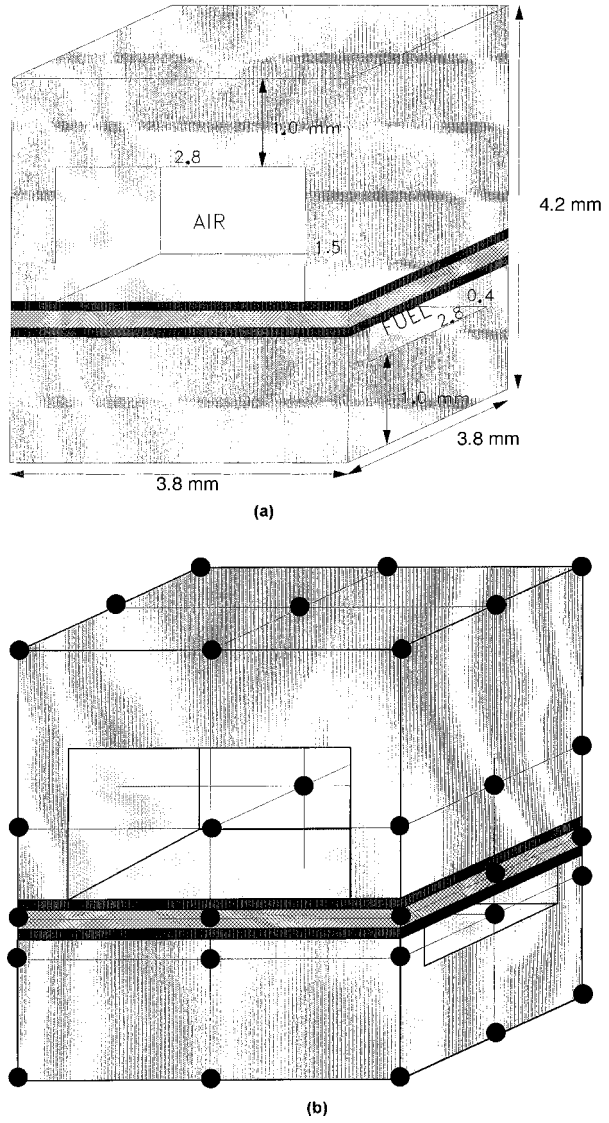

Fig. 1. (a) Typical unit cell geometry as the basic building block of a cross-flow SOFC stack and (b) its discretization into a minimum 45 mesh finite-difference network for rigorous numerical computation of the temperature distribution.

assumed to be split by an insulating plane through the 'triple layer', consisting of adjacent anode, electrolyte and cathode plates. Since the reaction heat is generated at, and dissipated away from the triple layer, this is a reasonable assumption. The anode and cathode compartments thus act as parallel resistive elements in the equivalent heat conduction circuit. Each half cell can in turn be represented by a series and parallel combination of resistive elements as shown in Fig. 2(b), in which R3 and R8 stand for cross-channel radiative transfer and the remainder for conduction in various solid elements.

Thus, for the cathode (air) half cell, the thermal resistance for heat flow across the gas channel, as indicated in Fig. 2, can be expressed as

$$R_{\text{air}} = \left[\frac{1}{R_2} + \frac{1}{R_3} + \frac{1}{R_4}\right]^{-1} + R_1 + R_5 \qquad (1)$$

in which the thermal resistances of the elements are approximately given by

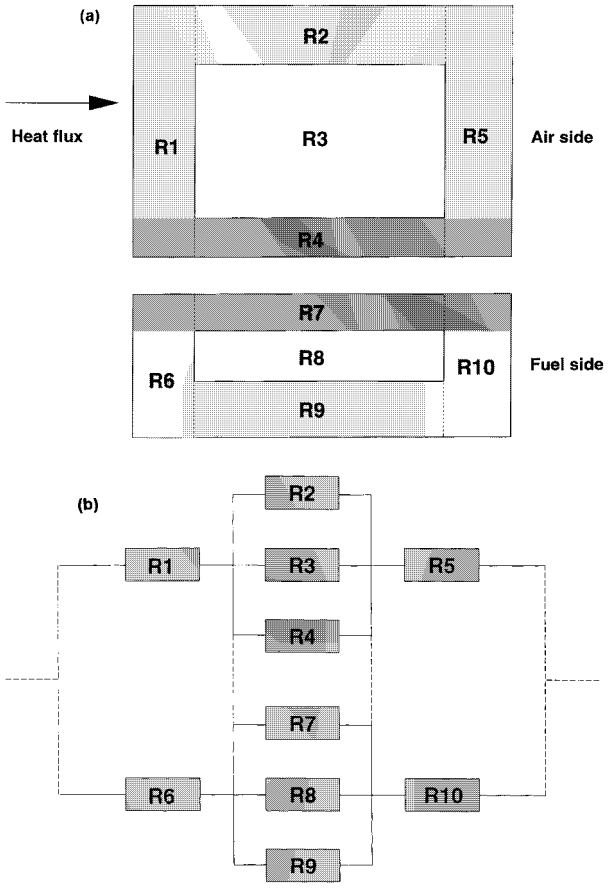

Fig. 2. (a) Casting of a unit cell cross section in terms of thermally resistive elements and (b) representation of the latter in terms of an equivalent circuit for heat conduction.

$$R_{\text{j}} = \frac{l_j}{k^{\text{o}} A_{\text{j}}} \qquad (2)$$

The radiative resistances are given by

$$R_j = \frac{1}{4F\sigma\varepsilon A_{\text{w}} T_{\text{j}}^3} \qquad (3)$$

The effective conductivity for the half cell, corresponding to heat flow across the channel, is obtained from the expression

$$k_{\text{air}} = \frac{l}{R_{\text{air}} A_{\text{c}}} \qquad (4)$$

Expressions for the effective conductivities for heat flow along the channel and vertical cross-channel directions are derived in a similar manner. For the former, the effect of radiation along the channel is neglected, and the effective conductivity is given simply by

$$k_{\text{air}} = k^{\text{o}} V_{\text{air}}^{\text{s}} \qquad (5)$$

Analogous equations are applicable to the anode (fuel) side.

By using the above formulae, the effective conductivity of the unit cell in all three directions of the coordinate system can be estimated. For coflow or counterflow configuration, for example, the effective conductivities across, and in the direction of, gas channels, respectively, are given by the following expressions:

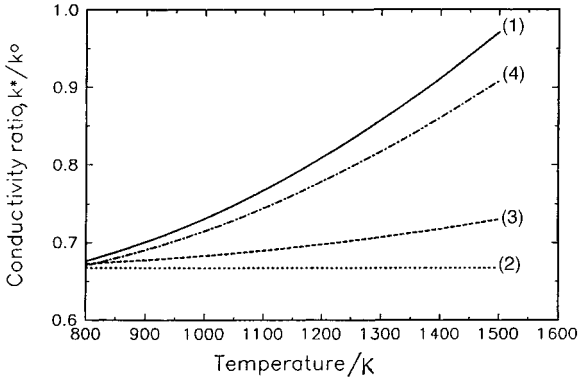

Fig. 3. Variation of effective conductivities as a function of temperature for $\varepsilon = 0.8$. Key: (1) perpendicular air direction co- or counterflow; (2) air direction co- or counterflow; (3) air direction cross flow; (4) fuel direction cross flow.

$$k_1^* = k_{\text{air}} V_{\text{air}}^{\text{o}} + k_{\text{fuel}} V_{\text{fuel}}^{\text{o}} \tag{6}$$

$$k_2^* = k^{\text{o}} \left(V_{\text{air}}^{\text{o}} V_{\text{air}}^{\text{s}} + V_{\text{fuel}}^{\text{o}} V_{\text{fuel}}^{\text{s}} \right) \tag{7}$$

In the cross-flow configuration, effective conductivities in the directions of air and fuel flow, respectively, are given by

$$k_3^* = k^{\text{o}} V_{\text{air}}^{\text{o}} V_{\text{air}}^{\text{s}} + k_{\text{fuel}} V_{\text{fuel}}^{\text{o}} \tag{8}$$

$$k_4^* = k_{\text{air}} V_{\text{air}}^{\text{o}} + k^{\text{o}} V_{\text{fuel}}^{\text{o}} V_{\text{fuel}}^{\text{s}} \tag{9}$$

Figure 3 shows the variation of effective conductivities as a function of unit cell temperature. The ratio k_2^*/k^{o} is independent of temperature since radiation along the channels is neglected. Emissivity of the solid, which is not usually accurately known, can be an important source of error in estimating the effective conductivities, as shown in Fig. 4 for k_1^*. The effective conductivities estimated in this manner are nearly identical to those estimated from more rigorous numerical calculations [3].

Together with the assumption that the solid and gas phase temperatures, as well as compositions, are uniform in the unit cell (CSTER assumption for the unit cell), this approach in effect eliminates the need for a detailed finite difference network for the unit cell, and allows the representation of a unit cell in terms of a single mesh point in the calculation of temperature distribution in the stack [3].

In a similar manner, the equations for current and potential distribution in the solid can be expressed in terms of an equivalent circuit. This is again based on identifying repeating geometrical segments of the solid, estimating the resistances of these analytically, and then combining these in series or parallel to obtain the equivalent circuit representing the flow of charge in the solid according to Ohm's law. These assumptions greatly simplify the numerical procedure without introducing significant errors to the numerical results relative to, for example, estimating the cell overpotential and the methane reforming rate which are the two important sources of uncertainty in such calculations.

4. Application to an experimental model

The experimental cell stack used for the validation of the model discussed above was constructed from commercial and laboratory produced components [4]. 200 mm thick YSZ (8Y) plates (dimensions 70 mm × 70 mm) were used as the electrolyte. Anode (60 vol % Ni and 40 vol % ZrO_2(8Y)) and cathode ($La_{0.5}Sr_{0.5}MnO_3$) thicknesses were 40 and 25 mm, respectively. The ceramic interconnectors were machined from $LaCrO_3$(Ca) plates to a cross-flow configuration. The assembled SOFC stack consisted of 14 cell plates fitted in an alumina tube as shown in Fig. 5. The open segments of the alumina tube between the sealed corners of the stack were utilized as fuel and air manifolds. Each cell plate consisted of 12 fuel and air channels. Some of the geometric details can be discerned from the unit cell sketch in Fig. 1.

The stack was operated in a furnace maintained at 1000 °C, and the feed gases were preheated to the same temperature before they were introduced into their respective manifolds. Air was fed into the cathode side at a flow rate of 4600 normal $cm^3\ min^{-1}$. The anode feed consisted of a mixture of methane and steam at the flow rates and 475 normal $cm^3\ min^{-1}$ and 712 normal $cm^3\ min^{-1}$, respectively. The details about the experimental study can be found elsewhere [4].

The fuel was assumed to enter the stack without any prereforming in the manifold. The reforming rate on the anode was estimated from the data of Parsons

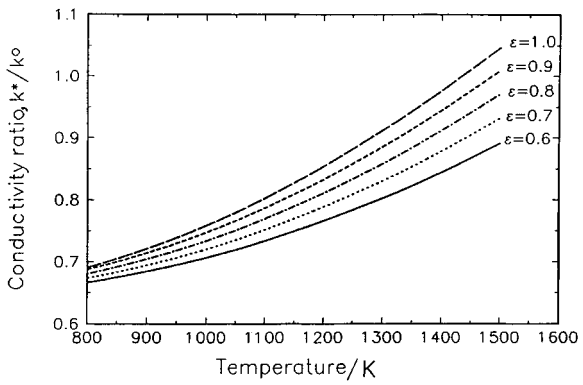

Fig. 4. Effect of solid emissivity on the calculated effective conductivity.

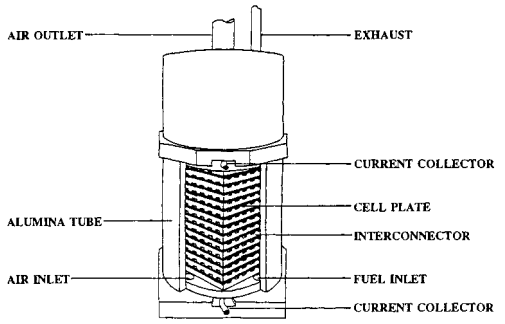

Fig. 5. Sketch of cell stack used in obtaining the experimental data [4]. The estimated active electrode area per cell plate is 33 cm^2.

and Randall [5]. The electrical conductivity of the cell components were based on the data reported in [4], and the thermal conductivity data for the interconnector material were obtained from Sakai *et al.* [6]. The sum of anodic and cathodic overpotentials and the contact resistances were estimated in the manner described previously [2] (pre-exponential factor assumed to be $8.5\,\Omega\,cm^2$). Following the calculations reported by Solheim [7], 50% of the electrode area covered by the interconnector ribs was assumed to be active. Feed gases were assumed to distribute into the stack channels at equal flow rates at the inlets.

Radiative heat transfer between the outer surface of the stack and the inner wall of the manifold was taken into consideration by assuming the vertical surfaces of the manifold to be at 1000 °C. It was assumed further that the top surface of the stack, which was not shielded against radiative heat transfer, radiated to a cooler outer surface at 900 °C, based on measurement of temperature distribution at the furnace walls. Heat losses from the bottom were neglected since the stack rested on a thermally well-insulated surface.

Figure 6 indicates a good agreement between the numerical results and experimental data obtained from a typical stack test under specified conditions. The discrepancy between the measured and predicted values becoming appreciable at high current outputs is probably a result of inadequate overpotential data under these conditions.

With added confidence thus gained in the software and data base, it was possible to obtain details of various distributions in the experimental cell under the specified operating conditions. Figure 7 shows the temperature and current distributions along the stack on a vertical plane at about the middle of the stack, indicating that the largest gradients in the vertical direction occur close to the stack top due to larger radiation losses there relative to the losses close to the bottom. However, the gradients in the horizontal direction become larger towards the bottom of the stack. This is due to domination of radiation losses from the vertical outer surfaces of the stack. In response to these temperature variations, the plate potentials, which change little close to the bottom, decrease as the stack top is approached, as shown in Fig. 8. It is worth noting that the top plate, which loses heat by radiation to a colder surface above, receives heat at the edges from the warmer vertical surface of the manifold. Therefore, the temperature at the edge can be higher than at the middle of the plate (Fig. 7(a)).

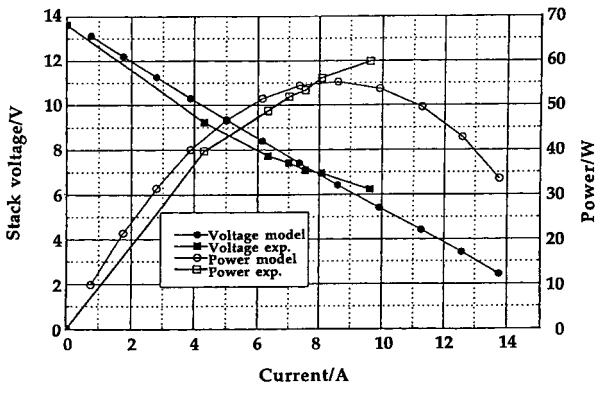

Fig. 6. Comparison of experimental [4] and calculated data for stack performance.

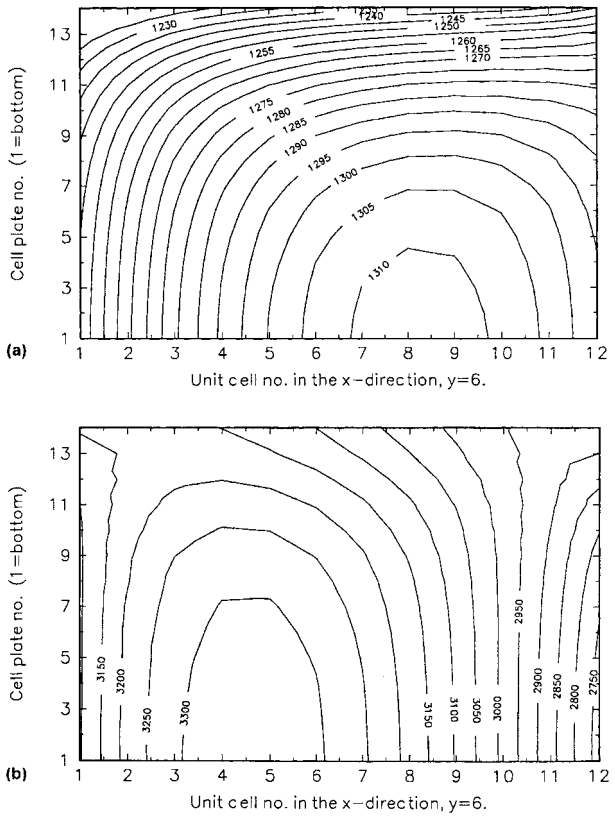

Fig. 7. Simulated (a) isotherms (K) and (b) current distribution ($A\,m^{-2}$) for the experimental stack at a vertical plane cut through the middle of the stack. Fuel flows from left to right and air perpendicular into the figure plane.

5. Conclusions

Mathematical models for simulating the performance of SOFC stacks have been developed to a stage where they are becoming useful engineering design tools. They are also useful in visualizing temperature, current and concentration distributions which are difficult to measure by experimental techniques. In this

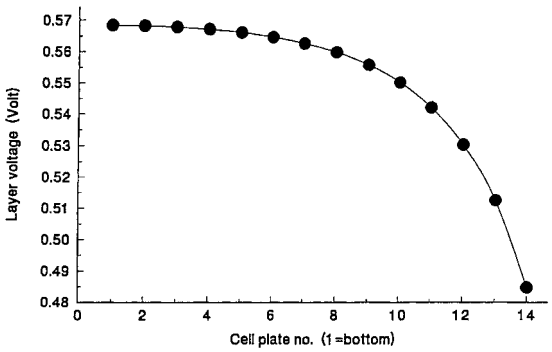

Fig. 8. Simulated potential distribution in the experimental stack.

respect, numerical simulations are proving pertinent tools for troubleshooting purposes. The mathematical SOFC model developed has so far proved to be useful for the planning of experiments, interpretation of experimental results, mapping out operating conditions, which may destroy an expensive experimental stack, and for designing and simulation of new stack designs. The main drawback in the applicability of such models is the uncertainty of input data, in particular electrochemical reaction and reforming rates. Development of separate models for these processes, based on kinetics and transport phenomena approaches, is in progress [9].

Acknowledgement

This work was supported by Statoil a.s.

References

[1] K. Nisancioglu, Proceedings of the 5th IEA Workshop: SOFC Materials, Process Engineering and Electrochemistry, 2–4 March 1993, Jülich, Germany (1993).

[2] H. Karoliussen, K. Nisancioglu, A. Solheim and R. Ødegård, Proceedings of the 3rd International Symposium on Solid Oxide Fuel Cells, Honolulu, Hawaii, The Electrochemical Society, Pennington, NJ (1993).

[3] H. Karoliussen, K. Nisancioglu and A. Solheim, Proceedings of the 5th IEA Workshop: SOFC Materials, Process Engineering and Electrochemistry, Forschungszentrum Jülich, Germany (October 1993), p. 245.

[4] H. Karoliussen, 'Matematisk modellering av fastoksid brenselcelle', Dissertation, Department of Electrochemistry, Norwegian Institute of Technology, Trondheim (1993).

[5] R. Ødegård, I.R. Theodorsen, T. Sigvartsen, T. Monsen and H. Løvåsen, *in* 'High Temperature Electrochemical Behaviour of Fast Ion and Mixed Conductors', Proceedings of 14th Risø International Symposium on Materials Science, Risø National Laboratory, Roskilde, Denmark (1993).

[6] J. Parsons and S. Randall, SOFC Micromodelling, IEA SOFC Task Report, Swiss Federal Office of Energy, Bern (May 1992).

[7] N. Sakai, T. Kawada, H. Yokokawa, M. Dokiya, and Y. Takahashi, Proceedings of 11th Japanese Symposium on Thermophysical Properties, Tokyo (1990), p. 207.

[8] A. Solheim, Proceedings of the 3rd International Symposium on Solid Oxide Fuel Cells, Honolulu, Hawaii, The Electrochemical Society, Pennington, NJ (1993).

[9] A. M. Svensson, S. Sunde and K. Nisancioglu, Proceedings of the 17th Risø International Symposium on Materials Science, High Temperature Electrochemistry: Ceramics and Metals (edited by F. W. Poulsen, N. Bonanos, S. Linderoth, M. Mogensen and B. Zachau-Christiansen) Risø National Laboratory, Roskilde, Denmark (1996), p. 431.